5774 *Chem. Mater.* **2010,** *22,* 5774–5779
DOI:10.1021/cm101594c

CHEMISTRY OF MATERIALS
Article

Comparisons between Haydeeite, α-$Cu_3Mg(OD)_6Cl_2$, and Kapellasite, α-$Cu_3Zn(OD)_6Cl_2$, Isostructural $S = 1/2$ Kagome Magnets

R.H. Colman, A. Sinclair,[†] and A.S. Wills*

Christopher Ingold Laboratories, Department of Chemistry, University College London, 20 Gordon Street, London, U.K., WC1H 0AJ. [†]*Present address: School of Chemistry, Joseph Black Building, West Mains Road, Edinburgh, U.K., EH9 3JJ.*

Received June 11, 2010. Revised Manuscript Received September 17, 2010

The search for new $S = 1/2$ kagome antiferromagnets has been an ongoing challenge for the researchers interested in frustrated magnetism. Intrigue has surrounded these materials since the proposal that the high frustration of the kagome antiferromagnet and quantum fluctuations could prevent the formation of conventional Néel order and allow the formation of the resonating valence bond (RVB) state at low temperatures. There remain relatively few examples of $S = 1/2$ kagome magnets with crystal structures that have 3-fold symmetry, as many feature distortions that lower the crystal symmetry to monoclinic and reduce the degeneracy of the kagome lattice. In this article, we detail the synthesis and preliminary magnetic investigations of a new quantum kagome magnet, haydeeite, α-$Cu_3Mg(OH)_6Cl_2$. Comparisons with the isomagnetic and isostructural analogue kapellasite, α-$Cu_3Zn(OH)_6Cl_2$, are discussed.

1. Introduction

Geometrically frustrated magnets provide important models for the investigation of systems with competing interactions and degenerate ground states. While experimental examples of classical frustrated magnets are well studied in 3-dimensional (3D)[1−6] and 2-dimensional (2D)[7−13] networks, there remain many questions over the roles frustration can play in conductors[14−16] and the $S = 1/2$ limit, where quantum fluctuations are strongest.[17−20] At present, particular attention has been directed toward 2D kagome antiferromagnets (KAFMs) with $S = 1/2$, as theoretical work has predicted that in these systems quantum effects and the low dimensionality can stabilize exotic ground states, such as the long sought after resonating valence bond (RVB) state, a key reference to the superconducting state of the high T_c cuprates.[21−23] Despite its importance, the RVB state has continued to elude experimental study, with its observation limited to subtle traits, such as minor modifications of the inelastic spectrum of the quantum magnet copper-formate-tetra-deuterate (CFTD).[24]

Experimental interest in spin liquids and the RVB state was recently invigorated by the proposal that the mineral herbertsmithite[25] (also known as Zn−paratacamite and γ-$Cu_3Zn(OH)_6Cl_2$) is a model $S = 1/2$ kagome antiferromagnet.[18] Synthetic herbertsmithite has been shown by muon spin rotation techniques to have no ordering transition down to 50 mK,[26] despite a large Weiss temperature,

*Corresponding author. E-mail: a.s.wills@ucl.ac.uk.

(1) Greedan, J. E. *J. Alloys Compd.* **2006**, *408*, 444.
(2) Wills, A. S.; Zhitomirsky, M. E.; Canals, B.; Sanchez, J. P.; Bonville, P.; Dalmas de Reotier, P.; Yaouanc, A. *J. Phys.: Condens. Matter*. **2006**, *18*, L37.
(3) Poole, A; Wills, A. S.; Lelievre-Berna, E. *J. Phys.: Condens. Matter* **2007**, *19*, 452201.
(4) Ruff, J. P. C.; Clancy, J. P.; Bourque, A.; White, M. A.; Ramazanoglu, M.; Gardener, J. S.; Qui, Y.; Copley, J. R. D.; Johnson, M. B.; Dabkowska, H. A.; Gaulin, B. D. *Phys. Rev. Lett.* **2008**, *101*, 147205.
(5) Petrenko, O. A.; Balakrishnan, G.; Paul, D. McK.; Yethiraj, M.; McIntyre, G. J.; Wills, A. S. *J. Phys.: Conf. Ser.* **2009**, *145*, 012026.
(6) Yavors'kii, T.; Enjalran, M.; Gingras, M. J. P. *Phys. Rev. Lett.* **2006**, *97*, 267203.
(7) Fak, B.; Coomer, F. C.; Harrison, A; Visser, D.; Zhitomirsky, M. E. *Euro. Phys. Lett.* **2007**, *81*, 17006.
(8) Wills, A. S. *Can. J. Phys.* **2001**, *79*, 1501.
(9) Wills, A. S.; Dupuis, V.; Vincent, E.; Hamman, J. *Phys. Rev. B* **2000**, *62*, R9264.
(10) Grohol, D.; Matan, K.; Cho, J.-H.; Lee, S. H.; Lynn, J. W.; Nocera, D .G.; Lee, Y. S. *Nat. Mater.* **2005**, *4*, 323.
(11) Wills, A. S.; Ballou, R.; Lacroix, C. *Phys. Rev. B* **2002**, *66*, 144407.
(12) de Vries, M. A.; Johal, T. K.; Mirone, A.; Claydon, J. S.; Nilsen, G. J.; Rønnow, H. M.; van der Laan, G.; Harrison, A. *Phys. Rev. B* **2009**, *79*, 045102.
(13) Simonet, V.; Ballou, R.; Robert, J.; Canals, B.; Hippert, F.; Bordet, P.; Lejay, P.; Fouquet, P.; Ollivier, J.; Braithwaite, D. *Phys. Rev. Lett.* **2008**, *100*, 237204.
(14) Yoshii, S.; Iikubo, S.; Kageyama, T.; Oda, K.; Kondo, Y.; Murata, K.; Sato, M. *J. Phys. Soc. Jpn.* **2000**, *69*, 3777.
(15) Taguchi, Y.; Oohara, Y.; Yoshizawa, H.; Nagaosa, N.; Tokura, Y. *Science* **2001**, *291*, 2573.
(16) Fenner, L. A.; Dee, A. A.; Wills, A. S. *J. Phys.: Condens. Matter* **2009**, *21*, 452202.
(17) Hiroi, Z.; Yoshida, H.; Okamoto, Y.; Takigawa, M. *J. Phys.: Conf. Ser.* **2009**, *145*, 012002.
(18) Shores, M. P.; Nytko, E. A.; Bartlett, B. M.; Nocera, D. G. *J. Am. Chem. Soc.* **2005**, *127*, 13462.
(19) Wills, A. S.; Henry, J.-Y. *J. Phys.: Condens. Matter* **2008**, *20*, 472206.
(20) Colman, R. H.; Ritter, C.; Wills, A. S. *Chem. Matter.* **2008**, *20*, 6897.
(21) Hastings, M. B. *Phys. Rev. B* **2001**, *63*, 014413.
(22) Waldtmann, Ch.; Everts, H.-U.; Bernu, B.; Lhuillier, C.; Sindzingre, P.; Lecheminant, P.; Pierre, L. *Eur. Phys. J. B* **1998**, *2*, 501.
(23) Bernu, B.; Lecheminant, P.; Lhuillier, C.; Pierre, L. *Phys. Scr.* **1993**, *T49A*, 192.
(24) Rønnow, H. M.; McMorrow, D. F.; Coldea, R.; Harrison, A.; Youngson, I. D.; Perring, T. G.; Aeppli, G.; Syljuasen, O.; Lefmann, K.; Rischel, C. *Phys. Rev. Lett.* **2001**, *87*, 037202.
(25) Braithwaite, R. S. W.; Mereiter, K.; Paar, W. H.; Clark, A. M. *Mineral. Mag.* **2004**, *68*, 527.
(26) Mendels, P.; Bert, F.; de Vries, M. A.; Olariu, A.; Harrison, A.; Duc, F.; Trombe, J. C.; Lord, J. S.; Amato, A.; Baines, C. *Phys. Rev. Lett.* **2007**, *98*, 077204.

 Published on Web 10/05/2010

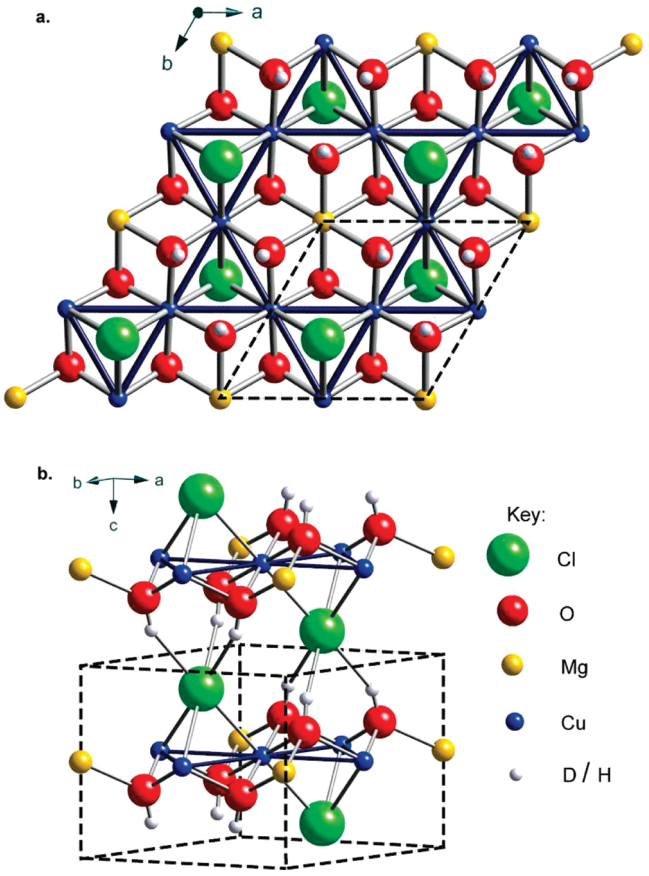

Figure 1. (a) In the ideal haydeeite structure, in space group $P3\bar{m}1$ (#164) is made up of a triangular array of metal ions that is segregated into non-Jahn−Teller distorted sites (occupied by Mg^{2+}) and a kagome lattice of the $S = 1/2$ Cu^{2+} ions. (b) The 2-dimensional planes are joined in the third dimension by weak interplanar O−H···Cl bonding (color online).

a clear sign of frustration; $\theta_w \approx -314$ K from bulk susceptibility measurements. Upon further examination, it has been shown that despite these promising properties, herbertsmithite cannot be considered a perfect KAFM due to an appreciable amount of antisite disorder between the diamagnetic Zn^{2+} and the $S = 1/2$ Cu^{2+} sites.[27] This disorder introduces coupling between the kagome planes, destroying the local 2-dimensionality of the system and creating defects similar to the local coordination of the Cu_4 end-member clinoatacamite γ-$Cu_2(OH)_3Cl$.[19,28−31]

Recently, a further member of the atacamite family was put forward as a model $S = 1/2$ KAFM, kapellasite, α-$Cu_3Zn(OH)_6Cl_2$.[20,32] Kapellasite is a newly discovered polymorph of herbertsmithite[33] and also contains a kagome network of $S = 1/2$ Cu^{2+} ions. However, whereas in herbertsmithite the 2D kagome network is formed from diamagnetic dilution of the 3D pyrochlore-like lattice of metals sites, in kapellasite, it is the result of ordered dilution of a triangular lattice by the Zn^{2+} (Figure 1). This leads to a crystal structure that is highly 2-dimensional, with coupling along the third dimension occurring only through weak interlayer O−H(D)···Cl hydrogen bonding.

In this paper, we report the synthesis and preliminary magnetic characterization of deuterated synthetic samples of haydeeite, α-$Cu_3Mg(OD)_6Cl_2$,[34] the magnesium analogue of kapellasite. We also present the neutron powder diffraction study of deuterated kapellasite, which allows comparison of the slight modifications in the crystal structure that arise when Mg^{2+} is used as the diamagnetic dopant, rather than Zn^{2+}. These materials, therefore, present opportunities for probing the effects of parameters, such as the Cu−O(H/D)−Cu bond angle and the hybridization of the bridging hydroxide group. Computational and theoretical work suggests that these structural parameters and the interactions that they mediate play a defining role in the nature of the magnetic groundstate.[23,35] The ability to test these predictions using real systems is key to understanding the physics of these highly sought after states.

2. Experimental Section

Deuterated haydeeite can be synthesized by adapting a method used for kapellasite, based on $MgCl_2$ solution and copper metal. Difficulties in the reproducibility of the reaction encountered during scaleup of both deuterated kapellasite and deuterated haydeeite syntheses led to the discovery that a nucleation surface was required for the isolation of pure phases over the more thermodynamically stable polymorphs herbertsmithite and Mg−paratacamite, respectively. Investigation of several sources of nucleation surface indicated that the addition of four ground glass beads, each with an approximate radius of 1 mm and a surface area of 12.5 mm^2, was optimal for isolation of these materials.

The final preparative conditions for deuterated kapellasite were as follows: copper powder (2.22 g, 35 mmol) was refluxed in a 0.25 M solution of $ZnCl_2$ in deuterium oxide (D_2O, 99.9 atom % D; 500 mL) with four ground glass beads (as a nucleation surface) and slow oxygen bubbling. After 15 min, a gray precipitate (identified as simonkollite by laboratory powder X-ray diffraction) had formed, and after 25 min, this precipitate quickly turned blue. The precipitate was collected by hot filtration under vacuum and washed with D_2O (3 × 50 mL) to minimize the formation of parasitic impurity phases. A suspension of the collected product in D_2O (50 mL) was sonicated (5 min) before allowing the unreacted copper to settle to the bottom (5 min). The top 40 mL of suspension was then collected, and the precipitate was isolated from suspension by centrifugation before drying under vacuum. The collected deuterated kapellasite (1.22 g) was found to be phase pure by laboratory X-ray diffraction (< 3 wt % parasitic impurity phase).

Deuterated haydeeite was synthesized from copper powder (2.22 g, 35 mmol) refluxed in a 3.5 M solution of $MgCl_2$ in D_2O

(27) Olariu, A.; Mendels, P.; Bert, F.; Duc, F.; Trombe, J. C.; de Vries, M. A.; Harrison, A. *Phys. Rev. Lett.* **2008**, *100*, 087202.
(28) Wills, A. S.; Raymond, S.; Henry, J.-Y. *J. Magn. Magn. Mater.* **2004**, *272−276*, 850.
(29) Lee, S.-H.; Kikuchi, H.; Qiu, Y.; Lake, B.; Huang, Q.; Habicht, K.; Kiefer, K. *Nat. Mater.* **2007**, *6*, 853.
(30) Zheng, X. G.; Kubozono, H.; Nishiyama, K.; Higemoto, W.; Kawae, T.; Koda, A.; Xu, C. N. *Phys. Rev. Lett.* **2005**, *95*, 057201.
(31) Zheng, X. G.; Kawae, T.; Kashitani, Y.; Li, C. S.; Tateiwa, N.; Takeda, K.; Yamada, H.; Xu, C. N.; Ren, Y. *Phys. Rev. B* **2005**, *71*, 052409.
(32) Janson, O.; Richter, J.; Rosner, H. *Phys. Rev. Lett.* **2008**, *101*, 106403.
(33) Krause, W.; Bernhardt, H.-J.; Braithwaite, R. S. W.; Kolitsch, U.; Pritchard, R. *Miner. Mag.* **2006**, *70*, 329.
(34) Schlüter, J.; Malcherek, T. *Neues Jahrb. Mineral., Abh.* **2007**, *184*, 39.
(35) Cepas, O.; Fong, C. M.; Leung, P. W.; Lhuillier, C. *Phys. Rev. B* **2008**, *78*, 140405.

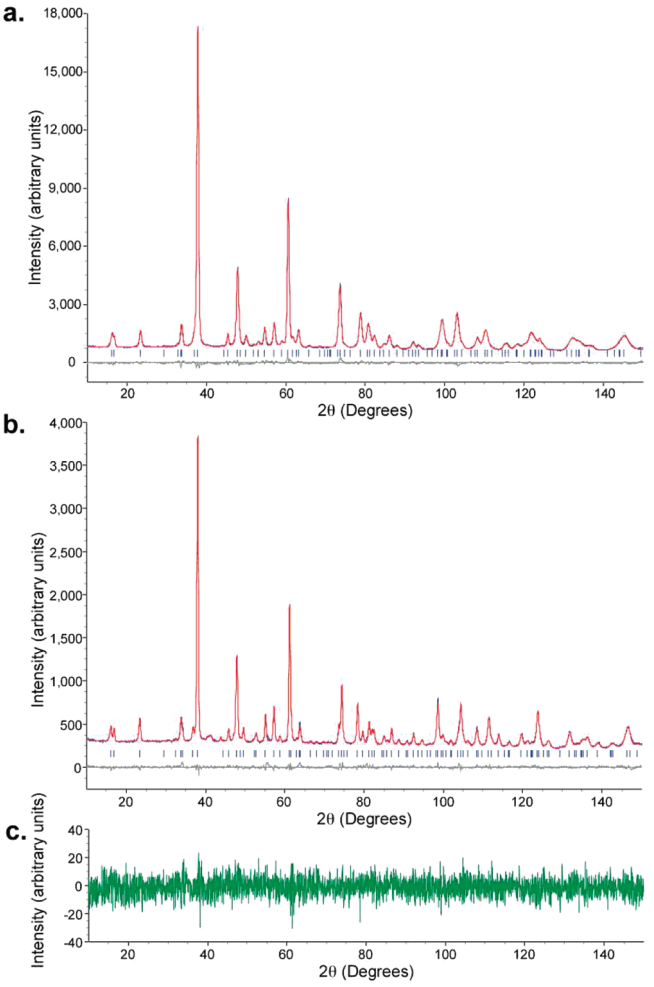

Figure 2. Rietveld refinement of diffraction spectra collected using neutrons of wavelength $\lambda = 1.6$ Å for (a) deuterated kapellasite (mass = 4 g, $T = 1.5$ K) and (b) deuterated haydeeite (mass = 0.6 g, $T = 1.5$ K). The blue, red, and lower lines represent the observed data, the calculated pattern, and the difference, respectively. Reflection positions are marked by the ticks. Final goodness-of-fit, χ^2, values were 2.693 (deuterated haydeeite) and 3.067 (deuterated kapellasite). (c) The low minus high temperature difference (1.5−6 K) between diffraction spectra collected from haydeeite shows no evidence for magnetic Bragg diffraction, despite the ferromagnetic transition observed in the susceptibility at $T_c = 4.2$ K (color online).

(500 mL) for 4 days with four ground glass beads and slow oxygen bubbling before a blue precipitate (haydeeite) had formed. The precipitate was then collected by hot filtration under vacuum and washed with D_2O (3 × 50 mL). A suspension of the collected product in D_2O (50 mL) was sonicated (5 min) before allowing the unreacted copper to settle to the bottom (5 min). The top 40 mL of suspension was then collected, and the precipitate was isolated from suspension by centrifugation before drying under vacuum. The collected haydeeite (0.692 g) was found to be phase pure by laboratory X-ray diffraction (< 3 wt % parasitic impurity phase).

Low temperature powder neutron diffraction (PND) data from deuterated haydeeite and kapellasite were collected using the D2b diffractometer at the ILL, Grenoble. The large sample masses required for PND were obtained by combination of multiple batches, after confirming identical structural parameters by laboratory X-ray diffraction. The samples were held

(36) TOPAS, program available from Bruker AXS GmbH, Östliche Rheinbruckenstrasse 50, 76187 Karlsruhe, Germany.

Table 1. Selected Bond Distances for Deuterated Kapellasite, $Cu_3Zn(OD)_6Cl_2$, and Haydeeite, $Cu_3Mg(OD)_6Cl_2$, at 1.5 K

	$Cu_3Zn(OD)_6Cl_2$	$Cu_3Mg(OD)_6Cl_2$
Cu−O	2.0075(19) Å	1.9866(16) Å
Cu−Cl	2.7009(30) Å	2.7470(22) Å
Zn/Mg−O	2.1202(25) Å	2.1137(23) Å
O−D	0.9987(65) Å	0.9838(53) Å
D−Cl	2.3932(52) Å	2.3472(42) Å

Table 2. Selected Bond Angles for Deuterated Kapellasite, $Cu_3Zn(OD)_6Cl_2$, and Haydeeite, $Cu_3Mg(OD)_6Cl_2$, at 1.5 K

	$Cu_3Zn(OD)_6Cl_2$	$Cu_3Mg(OD)_6Cl_2$
Cu−O−Cu	104.45(15)°	104.64(13)°
Cu−O−Zn/Mg	100.46(12)°	100.10(10)°
Cu−O−D	111.61(13)°	110.68(12)°
O−D−Cl	149.63(24)°	152.95(23)°
Cu−Cl−Cu	71.956(96)°	69.826(66)°
Cu−Cl−D	109.500(67)°	111.410(58)°
Cu−Cl−D	178.14(15)°	178.44(11)°

in vanadium cans, and the temperature was controlled using a standard cryostat. The low temperature experimental diffraction data and the pattern calculated using the Rietveld program TOPAS[36] are displayed in Figure 2a,b for deuterated samples of haydeeite and kapellasite. It was found that the 2D crystal structure of these materials led to anisotropic crystallite morphology and anisotropic peak widths. These could be successfully modeled by an eighth order spherical harmonic model for anisotropic peak broadening. The full refined structural data for these two materials are given in the Supporting Information, with selected bond lengths and angles given in Tables 1 and 2.

3. Results and Discussion

The refined structures were found to be highly deuterated, with a D/H ratio of >93%. Comparison of the crystal structures of herbertsmithite with haydeeite and kapellasite shows that the interlayer Cu−Cu distance is much smaller in herbertsmithite than in these quasi-2-dimensional materials (5.08 Å versus 5.73 Å and 5.68 Å, respectively); the intralayer Cu−Cu distances are also larger in herbertsmithite, 3.42 Å vs 3.15 Å and 3.17 Å.

The differences in coherent neutron scattering lengths of 3.631, 7.485, and 4.054 fm for Mg, Cu, and Zn respectively (for thermal neutrons), allowed the reliable refinement of occupancies of the two sites subject to the constraint that in both kapellasite and haydeeite the total metal site occupancies were fixed at unity. In the case of kapellasite, the 3*f* (kagome) site was found to be diluted by 26.8(40)% Zn^{2+} ions while the 1*b* site contains 11.6(36)% occupancy of Cu^{2+}. The refined Cu/Zn ratio of 1.37(12) is a notable deviation from the idealized Cu/Zn ratio of 3. The 3*f* (kagome) site of haydeeite shows considerably less mixing than kapellasite with 16.4(43)% Mg^{2+}, and the 1*b* site is refined to complete occupancy of Mg^{2+} in all cases, giving a Cu/Mg ratio of 1.68(18).

Consideration of the local coordination of the metal centers in terms of bond valence analysis[37] using the program VaList[38] did not yield any additional information about the level of segregation of the Jahn−Teller and

(37) Brown, I. D. *J. Appl. Crystallogr.* **1996**, *29*, 479.
(38) Wills, A. S. VaList, Program available from www.ccp14.ac.uk

Table 3. Comparison of the 3*f* (Kagome) Metal Site Environments in the Cu^{2+}/Zn^{2+} Kagome Systems Herbertsmithite and Kapellasite and Their Cu^{2+}/Mg^{2+} Analogues Mg−Herbertsmithite and Haydeeite[a]

site	bond	herbertsmithite[29]	Mg−herbertsmithite[39]	kapellasite	haydeeite
3*f*	M−Cl	2.763 Å	2.765 Å	2.703 Å	2.747 Å
	M−O	1.985 Å	1.988 Å	2.006 Å	1.987 Å
	<M−O(Cl)>	2.24 Å	2.25 Å	2.23 Å	2.24 Å
	M−Cl/M−O	1.392	1.391	1.347	1.382
1*b*	M−O	2.109 Å	2.100 Å	2.118 Å	2.114 Å

[a] A larger distortion, M−Cl/M−O, is indicative of greater occupation by the Jahn−Teller active Cu^{2+} ion and, therefore, of a higher segregation of the Cu^{2+} and $Zn^{2+}(Mg^{2+})$. Conversely, the coordination of the non-Jahn−Teller ion at the 1*b* site (MO_4) site is seen to vary little between the materials.

non-Jahn−Teller metal ions for both kapellasite and haydeeite; literature values for hebertsmithite and Mg-herbertsmithite are also presented for comparison (Table 3).[29,39] This lack of discrimination is unsurprising as the atomic radii of the different metals ($r(Mg^{2+})$ = 0.72 Å, $r(Cu^{2+})$ = 0.73 Å, and $r(Zn^{2+})$ = 0.74 Å)[40] and the values of <M−O(Cl)> are very similar for the 3*f* (kagome) sites. The same can be said of the nominally diamagnetic 1*b* site. There is, however, a variation in the ratio of the bond lengths, M−Cl/M−O, for the 3*f* site: its value is smallest for kapellasite, supporting the evidence that this material has the largest amount of the spherical diamagnetic ions on the kagome site. Haydeeite and two herbertsmithites feature larger ratios, suggesting that these materials have the largest proportions of Jahn−Teller active Cu^{2+} on the kagome site and that these are consequently the better model kagome magnets.

The magnetic interactions between the nearest-neighbor Cu^{2+} ions are mediated by two groups: the bridging μ_3-O(H/D) and μ_3-Cl^- units (Figure 1). The Cl^- ion lies on the 3-fold axis of the crystal structure, while the O(H/D) unit lies on a vertical mirror plane with the hydrogen bonding of the H/D to the Cl^- in the neighboring layer causing the O−H/D to cant away from the *c*-axis of the hexagonal structure. The details of the hybridization of these groups and that of the Cu^{2+} will play a critical role in determining the sign and strength of the various magnetic terms in the Hamiltonian. As well as the symmetric exchange (*J*), this could include antisymmetric exchange, the Dzyaloshinskii−Moriya (DM) interaction, which can play a defining role in the low temperature physics of kagome magnets.[35,41,42]

The values of the Cu−μ_3O(H/D)−Cu bond angle in haydeeite and kapellasite (104.7° and 104.4°, respectively) are close to the changeover in the sign of the superexchange found at 101−105° in several Cu−μ_3OH−Cu systems[21] and suggest that care must be taken when designating the interactions as being antiferromagnetic or ferromagnetic. Recent electronic calculations using the LDA and LSDA+*U* methodologies find that the nearest neighbor exchange integrals for kapellasite and haydeeite are antiferromagnetic and have magnitudes 2.5 and 0.8 meV, respectively.[32] The next strongest interactions are

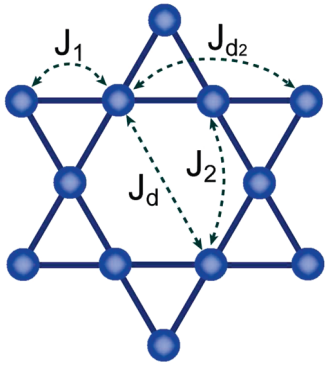

Figure 3. Magnetic interactions on the kagome lattice of kapellasite and haydeeite. J_d occurs through the Cu−O(H/D)−Zn/Mg−O(H/D)−Cu bridges.[32]

found to be those across the diagonals of the hexagons that make up the kagome network, J_d, (Figure 3) which are again antiferromagnetic (J_d = 0.9 and 0.8 meV for kapellasite and haydeeite, respectively). Interactions beyond these are sufficiently weak to be ignored (<0.5 meV). When considering the magnetic interactions in terms of the ratio $\alpha = J_d/J_1$, these electronic structure calculations indicate that J_d may play a more important role in haydeeite ($\alpha \approx 1$) than in kapellasite ($\alpha \approx 0.36$), though in both cases it could drive the systems toward the 12 sublattice order, predicted for competing further neighbor exchange interactions on the kagome lattice.[43] This last prediction has not been verified yet in kapellasite.

While the results of electronic structure calculations must be understood within the limitations of the technique, they do indicate that the contributions made to the valence band by the localized *d*-states of Zn and Mg are quite different, with those from Zn being greater than from Mg.[32] The exchange that these diamagnetic ions mediate within a more physically correct model can consequently be expected to be significantly different. It is clear that further work is needed to expand on these calculations, as their sensitivity to the type of ions that mediate J_d suggests that antisite disorder could play a pivotal role in defining the value of $\alpha = J_d/J_1$ in these materials and, consequently, the nature of their magnetic properties at low temperature.

Returning again to the crystal structures of kapellasite and haydeeite (Tables 1 and 2) we note that the O−D

(39) Colman, R. H.; Sinclair, A.; Wills, A. S., unpublished results.
(40) Shannon, R. D. *Acta Crystallogr.* **1976**, *A32*, 751.
(41) Elhajal, M.; Canals, B.; Lacroix, C. *Phys. Rev. B* **2002**, *66*, 014422.
(42) Ballou, R.; Canals, B.; Elhajal, M.; Lacroix, C.; Wills, A. S. *Phys. Stat. Sol. B* **2003**, *236*, 240.
(43) Domenge, J. C.; Sindzingre, P.; Lhuillier, C.; Pierre, L. *Phys. Rev. B* **2005**, *72*, 024433.

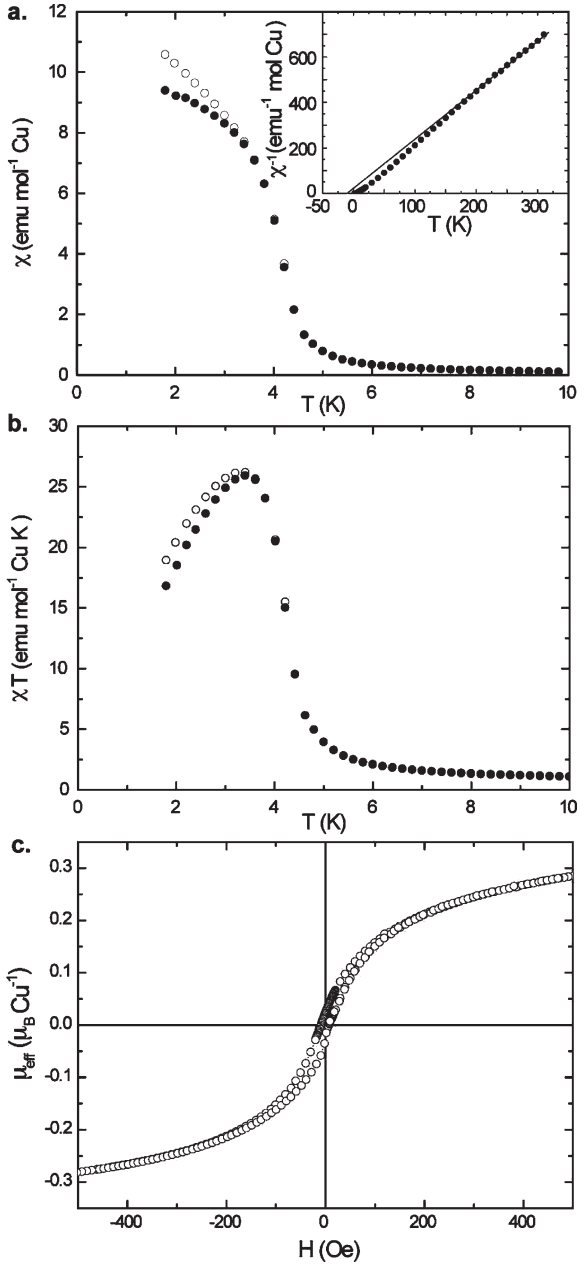

Figure 4. (a) dc susceptibility, χ_{dc}, of haydeeite at low temperature, with the temperature dependence of χ^{-1} shown in the inset; the full circles (●) represent the zero-field-cooled data, open circles (○) represent the field-cooled data. A ferromagnetic transition is clearly seen below $T = 4$ K, with the maximum in the derivative, $d\chi/dT$, at $T = 4.2$ K. (b) The temperature dependence of χT shows a downturn below $T = 3$ K indicating that there is an antiferromagnetic component involved in the ordering. (c) The field dependence of $\mu_{eff} = (8\chi T)^{1/2}$ at $T = 3$ K evidences a small hysteresis associated with the ferromagnetic transition and an extremely small spontaneous moment of $0.02\ \mu_B\ Cu^{1-}$.

bond lengths and Cu−O−D bond angles are very similar for the two materials. This finding contrasts with the short O−H bond (0.78 Å) determined by previous single crystal X-ray diffraction studies of a natural sample of haydeeite.[25] Taking the O−H (D) bond length and Cu−O−D(H) bond angles as indicators of the hybridization of the bridging μ_3-O(H/D) group, our refined structures do not point to the nearest neighbor exchange being qualitatively different in these isomorphic materials. In so doing, they support the hypothesis that another energy scale, such as the diagonal exchange J_d, is important in defining the differing magnetic properties of these materials.

In an effort to explore the differences between these $S = 1/2$ magnets and the roles played by the different crystallographic terms in the magnetism, we measured the magnetization of haydeeite using an MPMS-7 DC-SQUID magnetometer. A plot of χ vs T (Figure 4a) shows a magnetic transition below $T_c = 4.2$ K with a bifurcation of field-cooled from zero-field-cooled data. While the ferromagnetic nature of this transition is confirmed by the upturn below $T = 5$ K in χT vs T (Figure 4b), the observed decrease in χT below $T = 3.5$ K indicates that there is an antiferromagnetic component to the ordering process, as in a simple ferromagnet χT would saturate at low temperature. The near-zero value of the intercept on the temperature axis of χ^{-1} vs T indicates that these competing ferromagnetic and antiferromagnetic terms largely compensate what is considered as a mean field. Taking the Weiss temperature as zero, the high temperature region (200−300 K) could be well fitted to the Curie law with a Curie constant $C = 0.445(8)$ emu mol-Cu^{1-} and, hence, an effective moment $\mu_{eff} = 1.89\ \mu_B\ Cu^{1-}$. These values are slightly larger than expected from the spin only formula but are in good agreement with the values that can be derived for the observed Landé g-factors of similar $S = 1/2\ Cu^{2+}$ kagome systems.[44−46] The field dependence of the effective moment, μ_{eff}, (Figure 4c) at $T = 3$ K confirms the presence of a coherent ferromagnet component, showing typical form and hysteresis. The associated spontaneous moment is $0.02\ \mu_B\ Cu^{1-}$ (Figure 4c).

Questions over the nature of the low temperature magnetic ordering in haydeeite are fueled by the absence of any apparent Bragg scattering in the low temperature powder neutron diffraction data of haydeeite (Figure 2c). While such a small spontaneous moment would not be expected to be discernible in powder neutron diffraction data, there is also no evidence of antiferromagnetic long-range order. Exploration of simple trial models indicate that any ordered moment must be less than $0.4\ \mu_B\ Cu^{1-}$ to remain unobserved. Together with the small ferromagnetic moment observed by magnetometry, this points to the ground state of haydeeite below the 4.2 K transition remaining largely dynamic in nature, a reflection of the strong underlying frustration in this $S = 1/2$ kagome magnet.

4. Conclusion

In conclusion, we report the synthesis and preliminary magnetic characterization of haydeeite, a new $S = 1/2$ frustrated kagome magnet. Magnetization studies have shown haydeeite to undergo a transition below $T_c = 4.2$ K to a state that is dominantly ferromagnetic but does involve an antiferromagnetic contribution. The nontrivial

(44) Rigol, M.; Singh, R. P. *Phys. Rev. Lett.* **2007**, *98*, 207204.
(45) Hiroi, Z.; Hanawa, M.; Kobayashi, N.; Nohara, M.; Takagi, H.; Kato, Y.; Takigawa, M. *J. Phys. Soc. Jpn.* **2001**, *70*, 3377.
(46) Okamoto, Y.; Yoshida, H.; Hiroi, Z. *J. Phys. Soc. Jpn.* **2009**, *78*, 33701.

nature of the ordered magnetic structure is further evidenced by the failure to observe any peaks associated with long-range magnetic order below T_c in the powder neutron scattering spectra. The similarities between the low temperature nuclear structures of deuterated haydeeite and kapellasite support suggestions that the nature of the nominally diamagnetic metal ion site and the magnitude of the diagonal exchange J_d that it mediates are of crucial importance in these kagome magnets.

Acknowledgment. We thank the Royal Society and EPSRC (Grant Number EP/C534654) for financial support, the ILL for provision of neutron time, and C. Ritter for assistance with the experiment.

Supporting Information Available: Tables of the crystallographic parameters for the deuterated haydeeite and deuterated kapellasite samples (PDF). This material is available free of charge via the Internet at http://pubs.acs.org.